

Compression resistance of aluminium stub columns using Continuous Strength Method

M. Ashraf

School of Civil Engineering, The University of Queensland, St. Lucia, Australia

B. Young

Department of Civil Engineering, The University of Hong Kong, Hong Kong, China

ABSTRACT: Aluminium members are getting more popular in structural applications due to their high strength-to-weight ratio, corrosion resistance, attractive appearance, recyclability, ease of production and availability. The elastic modulus of aluminium, however, is only a third of ordinary steel, makes it vulnerable to excessive deflection. Thin sections are susceptible to local buckling at a relatively low stress and welding makes it even worse; the design stress i.e. 0.2% proof stress is almost halved in the vicinity of Heat Affected Zones (HAZ). Currently available design Codes have their guidelines both for welded and non-welded aluminium columns, which seem to produce conservative predictions for aluminium cross-sections subjected to compression. The current research aims to exploit a newly developed strain based design approach ‘Continuous Strength Method (CSM)’ to predict the behaviour of aluminium tubular cross-sections subjected to compression. This paper also explores the applicability of CSM to include the effects of HAZ.

1 INTRODUCTION

Aluminium tubular members have been used in structural engineering due to their high strength-to-weight ratio, lightness, corrosion resistance and ease of production. Aluminium members are generally manufactured by heat treated aluminium alloys to increase yield stress. The welding process, however, reduces the material strength significantly in a localized region, which is known as the Heat-Affected Zone (HAZ) softening. In the case of 6000 Series aluminium alloys, the heat generated from the welding can locally reduce the parent metal strength by as much as 68% (Zhu and Young, 2007). Aluminium structural elements could be connected to other parts by welding, which can adversely affect the structural performance. The current research investigates the available test results on aluminium stub columns reported by Zhu and Young (2006, 2007), Faella et al. (2000) and Langseth and Hopperstad (1999) to devise design principles following a recently developed strain based design concept the Continuous Strength Method (CSM).

2 THE CONTINUOUS STRENGTH METHOD

The basic notion of section classification of metallic thin-walled cross-sections based on the

width-to-thickness ratio of its constituent plate elements, originates from the yielding phenomenon observed in ordinary carbon steel. The success of this approach prompted its adoption for other metallic materials i.e. aluminium, high strength steel and stainless steel albeit the absence of any notable yielding phenomenon. The continuity in stress-strain behavior forms the basic concept for the Continuous Strength Method (Gardner, 2008), which was originally proposed for stainless steel (Gardner and Nethercot 2004, Ashraf et al. 2008) but its applicability to aluminium and high strength steel cross-sections were demonstrated elsewhere (Gardner and Ashraf, 2006).

The Continuous Strength Method (CSM) replaces the traditional cross-section classification by a continuous measure of cross-section slenderness β and cross-section deformation capacity ϵ_{LB} as defined by the following equations

$$\beta = \frac{b}{t} \sqrt{\frac{\sigma_{0.2}}{E_0}} \sqrt{\frac{4}{k}} \quad (1)$$

$$\epsilon_{LB} = \frac{\delta_u}{L} \quad (2)$$

where b = flat width of a plate element, t = thickness of the plate, $\sigma_{0.2}$ = 0.2% proof stress of the flat material, E_0 = Young's modulus of the material, k = plate buckling co-efficient, δ_u = axial

deformation corresponding to the peak load applied to a stub column (cross-section) and L = length of the stub column.

A continuous relationship is observed between the normalized deformation capacity ϵ_{LB}/ϵ_0 and cross-section slenderness β , which forms the basic design equation for CSM, where ϵ_0 = elastic strain at the 0.2% proof stress ($\epsilon_0 = \sigma_{0.2}/E_0$). Compound Ramberg-Osgood material model (Rasmussen 2001, Gardner and Ashraf 2006) is used to determine the local buckling stress σ_{LB} . The loss-of-effectiveness observed for slender cross-sections is incorporated into the CSM design equation to avoid the lengthy process of calculating effective area. In the case of stainless steel, the corner regions within a cross-section play significant role to enhance its resistance; these effects are also accounted for appropriately by incorporating a corner enhancement factor ϕ_c (Ashraf et al. 2008). Compression resistance $N_{c,Rd}$ of a cross-section is given by Equation 3, where A_g is the gross cross-sectional area.

$$N_{c,Rd} = \phi_c A_g \sigma_{LB} \quad (3)$$

Currently, the proposed CSM design equations for stainless steel include the effects of material nonlinearity in predicting bending resistance of cross-sections, flexural resistance of members and combination of actions (Ashraf et al. 2008, Gardner 2008). The current paper focuses on the compression resistance of aluminium stub columns and the inclusion of the effect of welding i.e. Heat Affected Zones (HAZ) in CSM.

3 CSM FOR ALUMINIUM CROSS-SECTIONS

3.1 Stub column tests

Basic design curves for aluminium and high strength steel were proposed by Gardner and Ashraf (2006) based on available results to demonstrate the applicability of CSM to nonlinear metallic materials other than stainless steel. Additional tests on slender cross-sections are now available (Zhu and Young, 2006 and 2007); these test results provide the chance to investigate the performance of CSM for very slender cross-sections. Table 1 summarises the test results used in the current study, whilst Figure 1 plots all the test results showing the variation in normalised deformation capacity ϵ_{LB}/ϵ_0 with cross-section slenderness β .

It is worth mentioning that the current study uses the flat width of the constituent plate elements, which is in line with available design codes; previously adopted concept of using centreline distances (Gardner and Ashraf, 2006) is thus modified.

Table 1. Tests on non-welded aluminium stub columns.

Reference	Cross-section type	No of stub columns	Range of β
Zhu and Young (2006)	SHS	1	1.89
	RHS	4	1.7–4.46
Faella et al. (2000)	SHS	24	0.33–1.95
	RHS	52	0.43–2.59
Langseth and Hoppersted (1997)	SHS	7	1.03–2.22

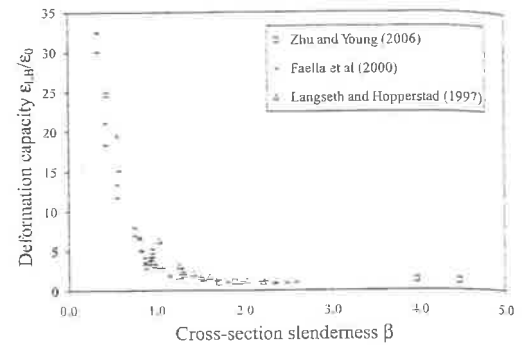


Figure 1. Test results for non-welded aluminium stub columns.

3.2 Design curve for aluminium stub columns

A total of 88 stub column test results are used herein to generate the design curve for aluminium cross-sections. Figure 2 shows the best fit curve based on the flat width of plate elements to determine β . The design equation is given in Equation 4.

$$\frac{\epsilon_{LB}}{\epsilon_0} = \frac{3.75}{\beta^{2.25-0.3\beta}} \quad (4)$$

The design curve proposed in Equation 4 does not include any modification to the deformation capacities for slender cross-sections, which was the case for all previously proposed CSM equations (Gardner and Nethercot 2004, Gardner and Ashraf, 2006, Ashraf et al. 2008). The loss of effectiveness in cross-sectional areas for slender cross-sections is an inevitable phenomenon due to local buckling and the concept is widely accepted. This effect was implicitly included in previously proposed CSM design equations for stainless steel, aluminium and high strength steel by modifying the deformation capacities of slender cross-sections. This implicit approach provides a simplistic analysis technique without going into the lengthy process of calculating effective areas. Recent discussions on CSM among researchers point out to the fact that it would be more

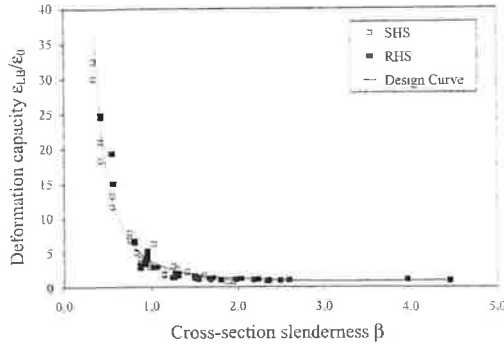


Figure 2. Design curve based on available test results.

appropriate to make explicit provisions for slender cross-sections. The current research hence adopts a different approach for slender cross-sections. The proposed design curve (Equation 4) has been used to predict the compression resistances of all cross-sections and the predictions are compared with the test results in Figure 3. It is obvious that the compression resistances for slender cross-sections are over-predicted largely due to the post-buckling effect, which is explained by Ashraf et al. (2008). It is worth noting that the test results reported by Zhu and Young (2006) allows to explore the validity of the method for very slender cross-sections although the design equation is dominated by the test results obtained from Faella et al. (2000).

Regression analysis was performed for slender cross-sections and it is proposed herein to use a coefficient ϕ_{eff} to explicitly take account of the loss-of-effectiveness for aluminium cross-sections with $\beta > 1.3$, which is equivalent to the Class 4 limit (slender cross-sections) in Euro Code 9 EN1999-1-1 (2007).

$$\phi_{\text{eff}} = -0.09\beta + 1.09 \quad (5)$$

3.3 Material model

The compound Ramberg-Osgood expression (Rasmussen 2001, Gardner and Ashraf 2006, Ashraf et al. 2008) is used in CSM to obtain the local buckling stress σ_{LB} by using the value of ϵ_{LB} obtained from the proposed design curve give by Equation 4. Since the Ramberg-Osgood (1943) material model is expressed in terms of stress, design tables, derived using the exact material model, were proposed to obtain σ_{LB} directly by knowing the value of corresponding ϵ_{LB} . Different tables are required for different grades as the stress-strain relationship changes with change in compound Ramberg-Osgood exponents n and m (Rasmussen, 2001) or $n'_{0.2,1.0}$ (Gardner and Ashraf 2006). Abdella (2006) proposed an approximate

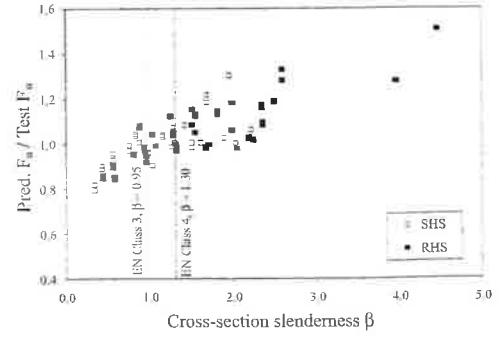


Figure 3. Comparison between test results and predictions using Equation 4.

inversion of the compound Ramberg-Osgood expression which enables obtaining σ_{LB} using the known value of ϵ_{LB} . The current research exploits the following formulations where the originally proposed notations are modified, where appropriate, to be consistent with those used in CSM. The σ_n and ϵ_n are normalised stress and strain respectively i.e. $\sigma_n = \sigma/\sigma_{0.2}$ and $\epsilon_n = \epsilon/\epsilon_{0.2}$, whilst $\epsilon_{0.2}$ is the total strain at $\sigma_{0.2}$.

$$\sigma_n = \frac{r \cdot \epsilon_n}{1 + (r-1) \cdot \epsilon_n^p} \quad \text{when } \epsilon < \epsilon_{0.2} \quad (6)$$

$$r = \frac{E_0 \epsilon_{0.2}}{\sigma_0} \quad (7)$$

$$r_{0.2} = \frac{E_{0.2} \epsilon_{0.2}}{\sigma_{0.2}} \quad (8)$$

$$p = \frac{r(1-r_{0.2})}{r-1} \quad (9)$$

$$\sigma_n = 1 + \frac{r_{0.2}(\epsilon_n - 1)}{1 + (r'-1) \left(\frac{\epsilon_n - 1}{\epsilon_{nu} - 1} \right)^{p'}} \quad \text{when } \epsilon > \epsilon_{0.2} \quad (10)$$

$$r' = \frac{E_{0.2}(\epsilon_u - \epsilon_{0.2})}{\sigma_u - \sigma_{0.2}} \quad (11)$$

$$r_u = \frac{E_u(\epsilon_u - \epsilon_{0.2})}{\sigma_u - \sigma_{0.2}} \quad (12)$$

$$p' = \frac{r'(1-r_u)}{r'-1} \quad (13)$$

$E_{0.2}$ and E_u are tangents at $\sigma_{0.2}$ and σ_u respectively. The expression for $E_{0.2}$, given in Equation 14, is readily available in relevant literature as it is obtainable from the original Ramberg-Osgood expression. Abdella (2006) proposed the following expression for E_u , as given in Equation 15.

$$E_{0.2} = \frac{E_0}{1 + 0.002n(E_0/\sigma_{0.2})} \quad (14)$$

$$E_u = \frac{E_{0.2}}{1 + (r' - 1)(1 + 3.5\sigma_{0.2}/\sigma_u)} \quad (15)$$

It is worth noting that E_u represents the slope of the stress-strain curve at the ultimate stress and hence it can be taken as 0 i.e. $E_u \approx 0$. This approximation makes $r_u = 0$ and thus $p' = r'/(r'-1)$, which clearly makes the material model relatively simple. These approximations do not significantly affect the final predictions for compression resistances, whilst makes the process relatively simple.

3.4 Proposed design method and comparisons

Following steps are hereby proposed to obtain the compression resistance for aluminium cross-sections:

- Determine the cross-section slenderness β for the most slender element using Equation 1 and find the local buckling strain ϵ_{LB} using the proposed design curve given by Equation 4.
- Obtain the local buckling stress σ_{LB} using either Equation 6 or Equation 10, whichever is appropriate.
- If the cross-section slenderness $\beta > 1.3$, determine ϕ_{eff} using Equation 5.
- Compression resistance of an aluminium cross-section $N_{c,Rd}$ is thus given by Equation 16.

$$N_{c,Rd} = \phi_{eff} \sigma_{LB} A_g \quad (16)$$

Predictions for the compression resistances of all considered test specimens are made using the proposed design method. A summary of the key parameters are given in Table 2 and Table 3 for Square Hollow Sections (SHS) and Rectangular Hollow Sections (RHS), respectively. The values for compound Ramberg-Osgood parameters n and n' are taken as 20 and 4.5 respectively; these values were reported for aluminium 6000 series by Gardner and Ashraf (2006). It should be noted that the compression resistances for the considered cross-sections were determined using the exact n values, where available, and the observed variation in overall prediction was less than 1%. This clearly points out that the proposed values of $n = 20$ and $n' = 4.5$ may safely be used in CSM for aluminium cross-sections when the exact values are not available. Further investigation is now underway to examine the effects of using different n values for different grades and how it affects the final member capacities.

The average predictions obtained from CSM demonstrates its accuracy and consistency for

Table 2. Predicted compression resistances for SHS aluminium cross-sections.

Reference Section	$\sigma_{0.2}$ N/mm ²	β	CSM F_u / Test F_u	EN F_u / Test F_u	
Zhu & Young (2006)	45 × 45 × 1.1	189	1.89	0.95	1.05
Faella et al. (2000)	15 × 15 × 1.0	214	0.33	0.79	0.70
	15 × 15 × 1.0	214	0.33	0.82	0.72
	40 × 40 × 4.2	224	0.42	0.90	0.83
	40 × 40 × 4.2	224	0.42	0.89	0.82
	50 × 50 × 3.1	223	0.83	1.04	0.98
	50 × 50 × 3.1	223	0.83	1.04	0.99
	50 × 50 × 4.3	203	0.55	0.93	0.85
	50 × 50 × 4.3	203	0.55	0.96	0.88
	70 × 70 × 4.1	176	0.75	0.97	0.89
	70 × 70 × 4.1	176	0.75	0.99	0.92
	80 × 80 × 4.3	194	0.87	1.01	0.95
	80 × 80 × 4.3	194	0.87	1.01	0.95
	100 × 100 × 3.9	210	1.28	1.08	1.04
	100 × 100 × 3.9	210	1.28	1.06	1.03
	60 × 60 × 2.3	158	1.15	1.04	1.01
	60 × 60 × 2.3	158	1.15	1.03	1.00
	80 × 80 × 2.1	187	1.95	1.19	1.11
	80 × 80 × 2.1	187	1.95	1.20	1.12
	100 × 100 × 6.0	294	0.98	0.96	0.91
	100 × 100 × 6.0	294	0.98	0.96	0.91
	150 × 150 × 4.9	209	1.50	0.94	0.87
	150 × 150 × 4.9	209	1.50	0.97	0.89
	150 × 150 × 5.1	258	1.68	1.14	1.03
	150 × 150 × 5.1	258	1.68	1.11	1.01
Langseth and Hop perstad (1997)	80 × 80 × 2.5	77	1.03	0.89	0.90
	80 × 80 × 2.0	77	1.30	1.03	1.01
	80 × 80 × 1.8	77	1.42	1.09	1.05
	80 × 80 × 2.5	115	1.26	0.98	0.99
	80 × 80 × 2.5	188	1.61	0.89	0.96
	80 × 80 × 2.0	188	2.03	0.84	0.91
	80 × 80 × 1.8	188	2.22	0.88	0.95
			Mean	0.99	0.94
			COV	0.09	0.11

aluminium cross-sections. CSM provides an overall 7% increase in compression resistance when compared with the predictions obtained using Eurocode 9 EN1999-1-1 (2007). Figure 4 and Figure 5 show the variation in predictions with cross-section slenderness β obtained using CSM and Eurocode 9 (2007) respectively.

4 EFFECT OF TRANSVERSE WELD ON COMPRESSION RESISTANCE

Zhu and Young (2006) reported a total of 8 stub column tests with transverse welds and subsequently

Table 3. Predicted compression resistances for RHS aluminium cross-sections.

Reference Section	$\sigma_{0.2}$ N/mm ²	β	CSM F_u /EN F_u / Test F_u	EN F_u / Test F_u	
Zhu & Young (2006)	100 × 44 × 1.3	196	3.96	0.94	0.75
	100 × 44 × 2.9	189	1.70	0.94	0.89
	100 × 44 × 1.3	260	4.46	1.04	0.71
	100 × 44 × 2.9	275	2.04	0.89	0.80
	100 × 44 × 2.9	275	2.04	0.89	0.80
Faella et al. (2000)	34 × 20 × 3.0	219	0.55	0.89	0.80
	34 × 20 × 3.0	219	0.55	0.91	0.81
	40 × 30 × 4.0	202	0.43	0.85	0.80
	40 × 30 × 4.0	202	0.43	0.86	0.82
	50 × 20 × 4.0	211	0.57	0.85	0.79
	50 × 20 × 4.0	211	0.57	0.84	0.78
	50 × 30 × 3.0	217	0.80	0.95	0.89
	50 × 30 × 3.0	217	0.80	0.96	0.90
	50 × 40 × 2.7	222	0.93	0.99	0.94
	50 × 40 × 2.7	222	0.93	0.98	0.93
	60 × 34 × 3.0	213	0.94	0.96	0.92
	60 × 34 × 3.0	213	0.94	0.96	0.92
	60 × 40 × 2.6	235	1.32	0.95	0.95
	60 × 40 × 2.6	235	1.32	0.96	0.96
	80 × 40 × 4.0	222	1.07	0.99	0.93
80 × 40 × 4.0	222	1.07	0.99	0.93	
100 × 40 × 4.0	217	1.28	1.05	1.02	
100 × 40 × 4.0	217	1.28	1.04	1.01	
120 × 50 × 4.2	216	1.50	1.04	1.01	
120 × 50 × 4.2	216	1.50	1.10	1.07	
150 × 40 × 4.1	225	1.98	0.97	0.89	
150 × 40 × 4.1	225	1.98	1.08	0.99	
180 × 40 × 4.2	212	2.18	0.92	0.84	
180 × 40 × 4.2	212	2.18	0.92	0.83	
100 × 50 × 4.0	216	1.31	0.97	0.98	
100 × 50 × 4.0	216	1.31	0.97	0.98	
60 × 40 × 2.2	220	1.54	1.00	0.99	
60 × 40 × 2.2	220	1.54	1.08	1.06	
60 × 40 × 2.2	220	1.54	1.07	1.05	
80 × 40 × 4.0	189	0.95	0.94	0.90	
80 × 40 × 4.0	189	0.95	0.92	0.87	
80 × 40 × 4.0	189	0.95	0.95	0.90	
80 × 40 × 2.1	225	2.23	0.91	0.87	
80 × 40 × 2.1	225	2.23	0.91	0.87	
60 × 40 × 2.0	234	1.67	0.93	0.86	
60 × 40 × 2.0	234	1.67	0.93	0.87	
100 × 25 × 2.3	265	2.59	1.10	1.00	
100 × 25 × 2.3	265	2.59	1.14	1.04	
120 × 60 × 2.7	210	2.34	1.04	0.97	
120 × 60 × 2.7	210	2.34	1.02	0.95	
200 × 100 × 4.9	235	2.35	0.96	0.89	
200 × 100 × 4.9	235	2.35	0.97	0.90	
47 × 40 × 2.9	251	0.87	1.08	1.02	
47 × 40 × 2.9	251	0.87	1.07	1.01	
180 × 70 × 4.6	320	2.48	1.04	0.91	

(Continued)

Table 3. (Continued)

Reference Section	$\sigma_{0.2}$ N/mm ²	β	CSM F_u /EN F_u / Test F_u	EN F_u / Test F_u	
180 × 70 × 4.6	320	2.48	1.03	0.90	
153 × 70 × 4.9	309	1.80	1.05	0.93	
153 × 70 × 4.9	309	1.80	1.07	0.95	
200 × 180 × 15	340	1.03	1.04	1.00	
200 × 180 × 15	340	1.03	1.04	1.00	
120 × 100 × 4.8	323	1.25	1.13	1.10	
120 × 100 × 4.8	323	1.25	1.12	1.09	
			Mean	0.99	0.92
			COV	0.08	0.10

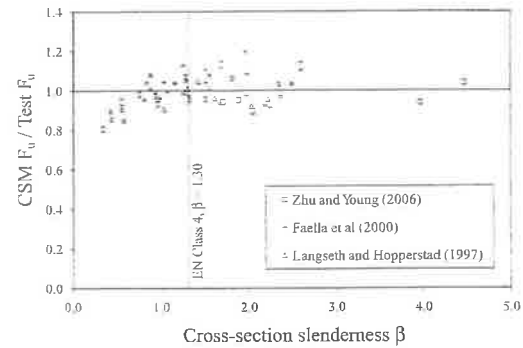


Figure 4. Predictions for compression resistance of aluminium stub columns using CSM.

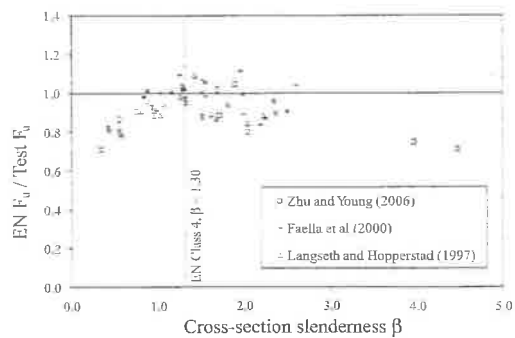


Figure 5. Predictions for compression resistance of aluminium stub columns using Eurocode 9 EN 1999-1-1 (2007).

verified the test results using finite element model developed using ABAQUS (Zhu and Young 2006a, 2006b). The obtained resistances were significantly lower than the corresponding non-welded stub columns, which is the obvious effect of Heat Affected Zone (HAZ) in the case of aluminium members.

Compression resistances obtained from tests were compared against those determined using Eurocode 9 EN1999-1-1 (2007), comparisons are shown in Figure 6. It is obvious that the predicted resistances are significantly conservative; Eurocode predicts only 68% of the test capacity with a coefficient of variation of 16% for the considered 16 stub columns including 8 results from FE analysis.

CSM is used herein to predict the resistances of aluminium stub columns with HAZ. Regression analysis led to a simple technique to achieve notable improvement in prediction. A new coefficient

$\phi_{HAZ} = 0.72$ is hereby proposed for use in case of stub columns with transverse web for the predictions by CSM. Thus the resistance $N_{c,HAZ}$ should be determined using Equation 17.

$$N_{c,HAZ} = \phi_{HAZ} N_{c,Rd} \quad (17)$$

Figure 7 compares the CSM predictions against the test and numerical results, which clearly shows significant improvement in overall agreement with a mean of 0.99 and a COV of 13%. Table 4 shows the key parameters for the considered stub columns.

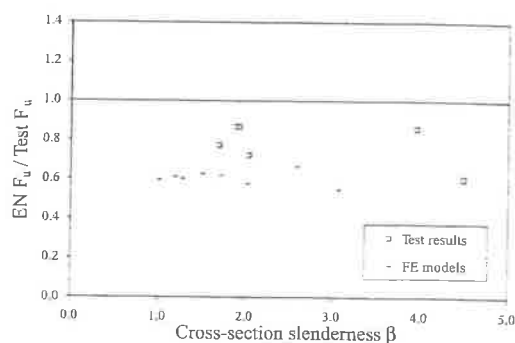


Figure 6. Predictions for compression resistance of welded aluminium stub columns using Eurocode 9 EN 1999 (2007).

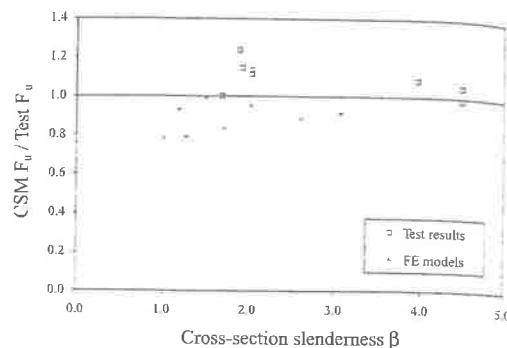


Figure 7. Predictions for compression resistance of welded aluminium stub columns using CSM.

Table 4. Predicted compression resistances for aluminium cross-sections with transverse welds.

Specimen	Section	$\sigma_{0.2}$ N/mm ²	β	CSM $F_u /$ Test F_u	EN $F_u /$ Test F_u
Test specimens	45 × 45 × 1.2	189	1.89	1.24	0.87
	45 × 45 × 1.1	189	1.92	1.15	0.87
	100 × 44 × 1.3	196	3.96	1.09	0.86
	100 × 44 × 2.9	189	1.69	1.00	0.78
	100 × 44 × 1.3	260	4.49	1.05	0.61
	100 × 44 × 1.3	260	4.49	0.99	0.61
	100 × 44 × 2.9	275	2.03	1.13	0.72
	100 × 44 × 2.9	275	2.03	1.11	0.72
FE specimens	204 × 204 × 4.0	189	2.59	0.88	0.67
	206 × 206 × 6.0	189	1.71	0.83	0.62
	208 × 208 × 8.0	189	1.27	0.79	0.60
	210 × 210 × 10	189	1.01	0.79	0.60
	204 × 204 × 4.0	275	3.06	0.91	0.55
	206 × 206 × 6.0	275	2.02	0.95	0.58
	208 × 208 × 8.0	275	1.50	0.99	0.63
	210 × 210 × 10	275	1.19	0.93	0.61
			Mean	0.99	0.68
			COV	0.13	0.16

5 CONCLUSIONS

Compression resistances for aluminium stub columns have been investigated in the current research to devise modified design equation following CSM technique; one of the significant modifications is the use of flat width of plate elements to determine cross-section slenderness β , which makes the approach consistent with available design Code provisions. To take appropriate account of slender cross-sections i.e. Class 4 sections in EN1999-1-1 (2007), explicit modifications are proposed by incorporating a coefficient ϕ_{eff} to include the effects of loss-of-effectiveness for cross-sections with $\beta > 1.30$. Inverted compound Ramberg-Osgood material model has been used to predict the local buckling stress σ_{LB} and simplifications to Abdella (2006) formulations have been proposed. Effects of compound Ramberg-Osgood coefficient has been studied and it is proposed to use the values of $n = 20$ and $n' = 4.5$ which produce good agreement if the exact values are not available. Overall predictions obtained using the proposed CSM equation for aluminium stub columns are more accurate and more consistent when compared with the Eurocode predictions.

In the current study, CSM has been also used to investigate the performance of aluminium stub columns with transverse weld. A very simple approach, incorporation of a new coefficient ϕ_{HAZ} produced significantly improved predictions for welded cross-sections. CSM provides an overall 45% increase in capacity for the considered welded stub columns with more consistent predictions.

ACKNOWLEDGEMENTS

The work described in this paper was supported by the William M.W. Mong Engineering Research Fund provided by The University of Hong Kong.

REFERENCES

- Abdella, K. (2006), Inversion of a full-range stress-strain relation for stainless steel alloys, *International Journal of nonlinear mechanics*, 41(3): 456–463.
- Ashraf, M., Gardner, L. and Nethercot, D.A. (2008), Structural stainless steel design: Resistance based on deformation capacity, *Journal of Structural Engineering ASCE*, 134(3): 402–411.

- Eurocode 9 EN 1999-1-1 (2007), Design of aluminium structures. General structural rules.
- Faella, C., Mazzolani, F.M., Piluso, V. and Rizzano, G. (2000), Local buckling of aluminium members: testing and classification, *Journal of Structural Engineering ASCE*, 126(3): 353–360.
- Gardner, L. (2008), The Continuous Strength Method, *Proceedings of the Institution of Civil Engineers, Structures and Buildings*, 161(SB3): 127–133.
- Gardner, L. and Ashraf, M. (2006), Structural design of nonlinear metallic materials, *Engineering Structures*, 28(6): 926–934.
- Gardner, L. and Nethercot, D.A. (2004), Structural stainless steel design: a new approach, *The Structural Engineer*, 82: 21–30.
- Langseth, M. and Hopperstad, O.S. (1997), Local buckling of square thin-walled aluminium extrusions, *Thin-Walled Structures*, 27: 117–126.
- Ramberg, W. and Osgood, W.R. (1943), Description of stress-strain curves by three parameters, Technical note No. 902, Washington (DC): National Advisory Committee for Aeronautics.
- Rasmussen, K.J.R. (2001), Full-range stress-strain curves for stainless steel alloys, Research report no 811, Department of Civil Engineering, University of Sydney, Australia.
- Zhu, J.H. and Young, B. (2006), Tests and design of aluminium alloy compression members, *Journal of Structural Engineering ASCE*, 132(7): 1096–1107.
- Zhu, J.H. and Young, B. (2006a), Aluminium alloy tubular columns—Part I: Finite element modelling and test verification, *Thin-Walled structures*, 44(9): 961–968.
- Zhu, J.H. and Young, B. (2006b), Aluminium alloy tubular columns—Part II: Parametric study and design using Direct Strength Method, *Thin-Walled structures*, 44(9): 969–985.
- Zhu, J.H. and Young, B. (2007), Effects of transverse welding on aluminium alloy columns, *Thin-Walled structures*, 45(3): 321–329.